Turkish Journal of Physics

http://journals.tubitak.gov.tr/physics/

Research Article

Turk J Phys
(2017) 41: 295 – 302

doi:10.3906/fiz-1612-2

Investigation of excitation functions of proton-induced reactions on ^{94,96,98,100}Mo targets for production of radioisotopes ^{94m,94g,96m,96g,96,99m}Tc

Ozan ARTUN, Hüseyin AYTEKİN*
Department of Physics, Bülent Ecevit University, Zonguldak, Turkey

Received: 01.12.2016 • **Accepted/Published Online:** 20.03.2017 • **Final Version:** 05.09.2017

Abstract: In this work, we investigated the excitation functions of proton-induced reactions on even–even $^{94-100}$Mo isotopes for the production of medical radioisotopes ^{94m,94g,96m,96g,96,99m}Tc. To obtain the excitation functions we carried out cross-section calculations in the frameworks of the generalized superfluid model, microscopic level density model, and three options of the preequilibrium process in the Talys code. The aim of this study was to introduce a new aspect for the production of radioisotopes ^{94m,94g,96m,96g,96,99m}Tc with different models.

Key words: Nuclear reaction models and methods, molybdenum, compound nucleus, radioisotope production

1. Introduction

Natural Mo isotopes are widely used for target materials to produce some medical radioisotopes, structural materials in nuclear reactors, nuclear energy equipment, and other radiation-proof devices. The ^{92,94,96,98,100}Mo isotopes are in abundances of 14.84%, 9.25%, 16.68%, 24.13%, and 9.63%, respectively [1]. In industrial and scientific research, in addition to being an alloying element, Mo is important in terms of being used as a pure construction material. Nowadays, obtaining theoretical data with reaction models is of particular importance along with the experimental data for radioisotope production by investigation of excitation functions [2]. The reason for this is that the excitation function values can be used for the impurity level and the integrated yield calculations in suggestions of reactions for radioisotope production [3].

Here we briefly present the fields of usage of the radioisotopes ^{94m,94g,96,96m,96g,99m}Tc, some of which are used in single photon emission computer tomography (SPECT) and positron emission tomography (PET). The radioisotopes ^{94g}Tc and ^{94m}Tc are used in PET [4]; in particular, the radionuclide ^{94m}Tc is properly used because of its β^+ decay property (E^+_β = 2.47 MeV) [5]. The radioisotopes ^{96}Tc and ^{96m}Tc are used as tracer isotopes in wear measurements [6] and ^{96g}Tc is used as a potential beam monitor [7]. Additionally, the radionuclide ^{96g}Tc was suggested for myocardial blood flow studies [8] and the prevention of coronary restenosis [7,9]. The most significant radionuclide for the major body organs in diagnosis is ^{99m}Tc [10,11], which causes minimal radiation dose to the patient and it is most widely used as a radiotracer in nuclear medicine [12].

In the present work, we aimed to explain suitable cross-section data, which are important for impurity levels and integrated yields, for the production of radioisotopes ^{94m,94g,96,96m,96g,99m}Tc. Therefore, we investigated the excitation functions of proton-induced reactions with different incident energy ranges. In

*Correspondence: huseyinaytekin@gmail.com

the calculation of cross sections, to suggest suitable data for radioisotope production, we used nuclear reaction models such as three pre-equilibrium (PEQ) models; generalized superfluid model (GSM), which is better than the standard Fermi-gas model (FGM) with constant temperature [3]; and microscopic level density (MLD) model. This study is also a part of Ozan Artun's PhD thesis [13].

2. Theoretical basis and codes

The PEQ reaction mechanism can be explained by the two-component exciton approach [14–16], which includes the FGM [3,14], GSM, and MLD model. We made the calculation with the Talys 1.6 code [17].

2.1. Exciton models

The PEQ model, which has an important mechanism, takes place between the direct process (10^{-22} s–10^{-20} s) and compound process (10^{-18} s–10^{-16} s) [18,19]. The basis of PEQ is Griffin's exciton model, which provided the first explanation of the spectral shapes of those pre-equilibrium particles [20]. This model was also used in order to investigate the particle energy spectra and excitation functions. In Griffin's exciton model, the state density statement is important because it explains the excitation function according to particle-hole state [21]. In accordance with this model, it was assumed that the system reaches equilibrium through a series of two-body interactions by causing transitions between particle-hole states. The Talys code simulates the nuclear reactions, and it can be used for cross-section calculations in the frame of the two-component exciton model [22], which was more developed the Griffin's exciton model (one-component) [18]. We used three modes, which are preeqmode 1–3, in calculations. The difference between preeqmode 1 and preeqmode 2 is the relation of the analytical and numerical calculations of transition rates, which are energy-dependent matrix elements. The preeqmode 3 is used for numerical transition rates with an optical model to calculate the collision probability [14]. The PEQ differential form for any particle k with emission energy E_k and with an emission rate W_k is given as

$$\frac{d\sigma_k^{PEQ}}{dE_k}=\sigma^{CF}\sum_{p_\pi=p_\pi^0}^{p_\pi^{max}}\sum_{p_v=p_v^0}^{p_v^{max}} W_k\left(p_\pi,h_\pi,p_\nu,h_\nu,E_k\right)\tau\left(p_\pi,h_\pi,p_\nu,h_\nu\right)\times P\left(p_\pi,h_\pi,p_\nu,h_\nu\right). \quad (1)$$

In this equation, σ_{CF}, P, p, h, and n are compound formation cross section, the part of the pre-equilibrium population, particle number, hole number, and exciton number (n = p + h), respectively. The π and ν represent the proton and neutron, respectively [14].

2.2. Level density models

The excitation function calculations were performed with two different level density models. These models are the MLD model and GSM. Detailed information about the GSM is given in the literature [3,14,23,24]. In addition to phenomenological models in the literature, we can use the MLD model via the Talys code in the excitation function calculations. The MLD model, which includes parity, spin (up to J = 30), and excitation energy (up to 150 MeV), uses Goriely's table [25] for Skyrme force. The MLD, which can be called ρ_{HFM}, is given by

$$\rho\left(E_x,J,\pi\right)=\exp\left(c\sqrt{E_x-\delta}\right)\rho_{HFM}\left(E_x-\delta,J,\pi\right), \quad (2)$$

where δ and c are pairing shifts and constant, respectively [14] and the HFM in ρ_{HFM} can be explained as the Hartree–Fock microscopically due to Hartree–Fock calculations.

3. Results and discussion

In this paper, we calculated the excitation functions of proton-induced reactions for production of the radioisotopes ^{94m,94g,96m,96g,96,99m}Tc with reaction models, which are the preeqmode 1–3, GSM, and MLD model. The calculated results were compared with the experimental data in the literature. The calculated E-threshold and Q-value of reactions are shown in the Table along with the decay data of the product radionuclides, which were taken from the EXFOR database [26].

Table. The calculated Q- value and E-threshold energy together with decay data [2,5,7,39,40] of the product radionuclides.

Nuclide	$T_{1/2}$	Mode of decay (%)	$E_\gamma(keV)$	$I_\gamma(\%)$	Reactions	Q-value (MeV)	E-threshold (MeV)
^{94m}Tc	52.5 min	IT(<0.1)	992.75	2.3	^{94}Mo(p,n)	–5.113601	5.168452
			1521.56	4.5	^{96}Mo(p,3n)	–21.637032	21.864284
^{94g}Tc	4.883 h	EC (100)	871.097	99.9	^{94}Mo(p,n)	–5.038101	5.092142
					^{96}Mo(p,3n)	–21.561532	21.787991
^{96m}Tc	51.5 min	IT(98)	778.196	1.9	^{94}Mo(p,n)	–3.789876	3.829680
		EC (2)	1200.16	1.09	^{98}Mo(p,3n)	–19.253745	19.451833
^{96g}Tc	4.28 d	EC (100)	778.196	99.76	^{94}Mo(p,n)	–3.755596	3.795040
			812.54	82	^{98}Mo(p,3n)	–19.219465	19.417200
			849.89	98			
			1126.83	15.2			
^{96}Tc	4.16 d	β^+	568.80	0.92	^{96}Mo(p,n)	–3.755596	3.795040
			778.22	100	^{98}Mo(p,3n)	–19.219465	19.417200
			812.58	82			
			849.93	97.6			
			1126.97	15.2			

3.1. Production of the radioisotopes ^{94m,94g}Tc

The calculated excitation functions of radioisotopes ^{94m,94g}Tc produced by (p,n) and (p,3n) reactions and all the experimental data are given in Figures 1–4. The results of the five nuclear models' calculations for the ^{94}Mo(p,n)^{94m}Tc reaction, namely preeqmod 1–3, GSM, and MLD model, and the experimental data from Rosh and Qaim, [27], Levkoskij [28], Skakun et al. [29] are shown in Figure 1. All the calculated results are close to the data reported by Skakun et al. and Rosh and Qaim up to 8 MeV from 6 MeV; however, beyond 8 MeV, the experimental cross-section results are higher than the calculated results. For the ^{96}Mo(p,3n)^{94m}Tc reaction (Figure 2), the data reported by Levkovskij [28] and Hogan [30] are in agreement with the calculated results at only about 25 MeV. Although the model calculations around the maximum values underestimate the experimental results by a factor of about 3, the experimental and model results have the same trend, and their maximum values are at about the same energies (30 MeV). The ^{94}Mo(p,n)^{94g}Tc reaction is presented in Figure 3 with the measurements reported by Rosh and Qaim [27], Levkovskij [28], and Skakun et al. [29]. For this reaction, from the threshold energy of the reaction to the maximum of the cross section, all the experimental results are lower compared to all of the calculated cross-section results and the experimental values are concentrated between 14 MeV and 19 MeV in which the experimental results are consistent with each other. In this energy range, the theoretical results are almost the same and close to the experimental

results especially with the GSM, but compared to the other theoretical results, the curve of the MLD model is far from the experimental results. The excitation function calculations of the ^{96}Mo(p,3n)^{94g}Tc reaction and the experimental results reported by Levkovskij [28] and Hogan [30] are presented in Figure 4. As seen, the model calculations are in reasonable agreement with the experimental data. As is also clearly visible in Figure 4, the calculation with the GSM are in good agreement with the results reported by Levkovskij [28] up to 29 MeV, but beyond the maximum of the excitation function the data reported by Levkovskij [28] do not have data points. For this reaction, the excitation function curve of the data reported by Hogan [30] is close to the excitation functions of the model calculations. However, while the excitation functions of preeqmode 1 and preeqmode 2 agree with the data reported by Hogan [30] (only one data point about 34 MeV), the calculation for the MLD model showed agreement with three data points beyond 39 MeV.

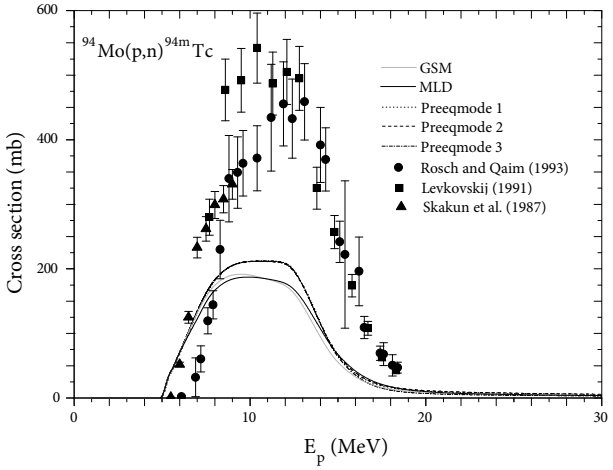

Figure 1. Comparison of excitation function of the ^{94}Mo(p,n)^{94m}Tc reaction with experimental data [27–29].

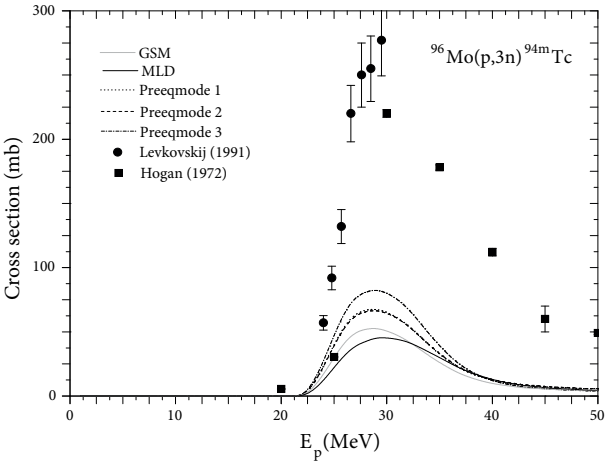

Figure 2. Comparison of excitation function of the ^{96}Mo(p,3n)^{94m}Tc reaction with experimental data [28,30].

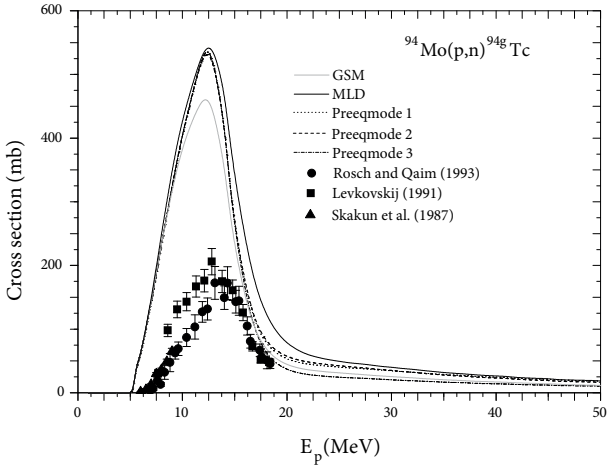

Figure 3. Comparison of excitation function of the ^{94}Mo(p,n)^{94g}Tc reaction with experimental data [27–29].

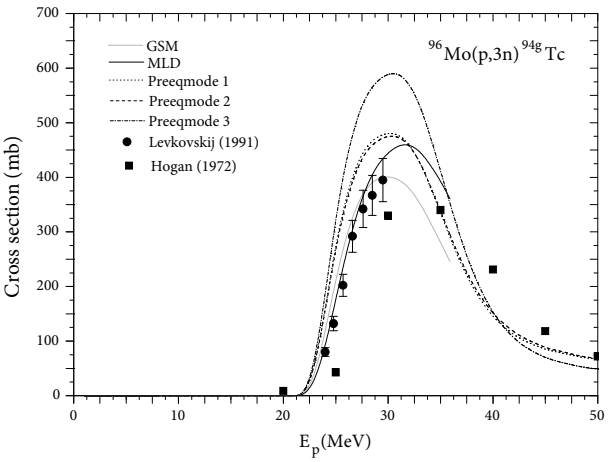

Figure 4. Comparison of excitation function of the ^{96}Mo(p,3n)^{94g}Tc reaction with experimental data [28,30].

3.2. Production of the radioisotopes ^{96m,96g,96}Tc

We presented the calculated excitation functions with the experimental data for the production of radioisotopes ^{96m,96g,96}Tc in Figures 5–8. The excitation functions for the production of radioisotope ^{96}Tc were derived by (p,n) and (p,3n) reactions. The theoretical excitation functions and the experimental results reported by Levkovskij [28], Flynn et al. [31], and Hogan [30] for the ^{96}Mo(p,n)^{96}Tc reaction are shown in Figure 5. The calculations of the experimental data described by Flynn [31] are rather good, but the data reported by Hogan [30] for this reaction is rather scanty beyond 8 MeV. The model calculations are somewhat lower than the measurements given by Levkovskij [28]. However, the results of the theoretical calculations are close to the measurements reported by Levkovskij [28] beyond the maximum of the excitation function. The excitation function calculations for the ^{98}Mo(p,3n)^{96}Tc reaction are shown in Figure 6 and this reaction was reported in one of the experimental results by Levkovskij [28]. On the other hand, the measured data points do not satisfy in the energy range above 30 MeV. The agreement between theoretical results and the data reported by Levkovskij [28] are good beyond the threshold energy and up to 27 MeV, but in the maximum of the excitation function, the model calculations and experimental data are separated from one another. The excitation function of model calculations and all experimental data reported for ^{96}Mo(p,n)^{96m}Tc and ^{96}Mo(p,n)^{96g}Tc reactions are given in Figures 7 and 8, respectively. For the ^{96}Mo(p,n)^{96m}Tc reaction, the results of model calculations are in agreement with each other and with all of the experimental data [29,30, 32] up to 7 MeV. In particular, the measurement by Zhuravlev et al. [32] agrees fairly well with all the model calculations. The measurement by Hogan [29] for this reaction is rather scanty (only five data points up to 30 MeV). The calculated excitation functions of the ^{96}Mo(p,n)^{96g}Tc reaction and the measurement by Hogan [30] are shown in Figure 8. Beyond 15 MeV, although there is a slight difference, the theoretical results agree with each other and the model calculations described the data reported by Hogan [30] rather well, except for one data point about 10 MeV. In the case of the ^{98}Mo(p,3n)^{96m}Tc and ^{98}Mo(p,3n)^{96g}Tc reactions, the literature has no data reported or the measurement for comparison with model calculations; however, the calculated E-threshold and Q-value of these reactions were added to the Table.

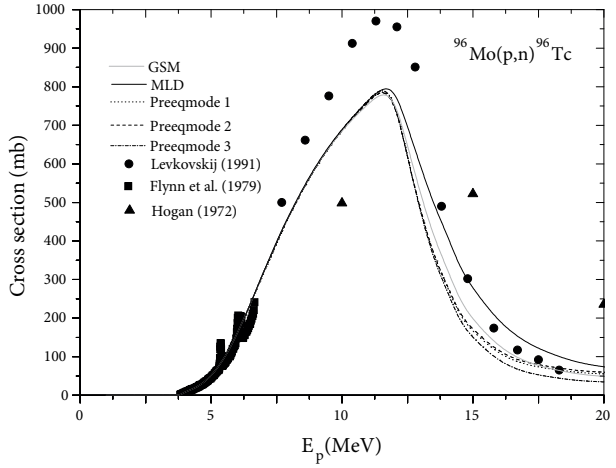

Figure 5. Comparison of excitation function of the ^{96}Mo(p,n)^{96}Tc reaction with experimental data [28,30,31].

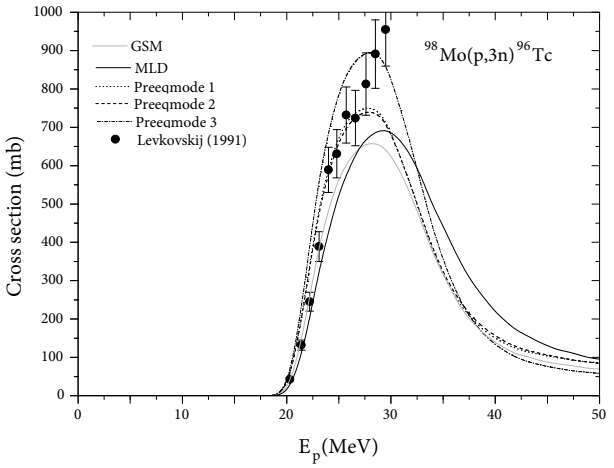

Figure 6. Comparison of excitation function of the ^{98}Mo(p,3n)^{96}Tc reaction with experimental data [28].

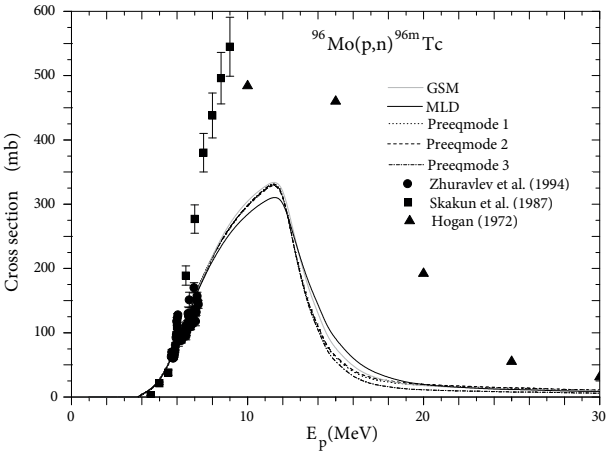

Figure 7. Comparison of excitation function of the ^{96}Mo(p,n)^{96m}Tc reaction with experimental data [29,30,32].

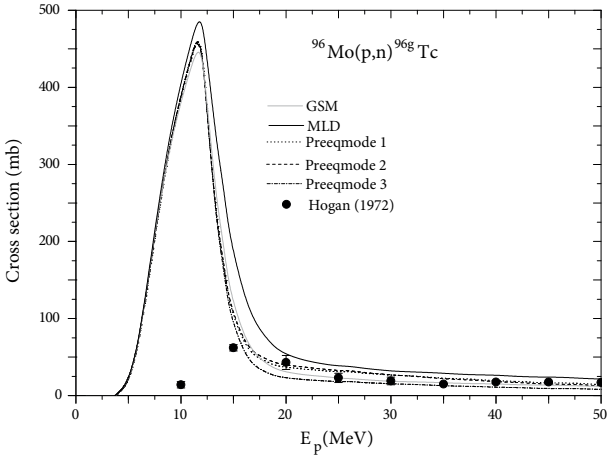

Figure 8. Comparison of excitation function of the ^{96}Mo(p,n)^{96g}Tc reaction with experimental data [30].

3.3. Production of the radioisotope ^{99m}Tc

The excitation functions, E-threshold, and Q value for the radioisotope ^{99m}Tc produced by three different reactions are given in the Table. The calculated excitation functions with the experimental data for (p,γ), and (p,2n) reactions are shown in Figures 9 and 10. The experimental data [33,34] and the model calculations for the ^{98}Mo(p,γ)^{99m}Tc reaction are shown in Figure 9. As seen, there are two peaks, which are at 2 MeV and about 12 MeV proton incident energies. The data reported by Sauter and Kappeler [34] are in good agreement with the theoretical results. However, there is a high error rate in the measurement by Scholten et al. [33]. When this error rate is considered, the theoretical results are in agreement with the measurement by Scholten et al. [33]; on the other hand, the cross section value for this reaction is too low ($<$0.4 mb). The results of nuclear model calculations together with ten experimental data for the ^{100}Mo(p,2n)^{99m}Tc reaction are shown in Figure 10. The data reported by Levkovskij [28], Lagunas-Solar et al. [35], Challan et al. [36], and Gagnon

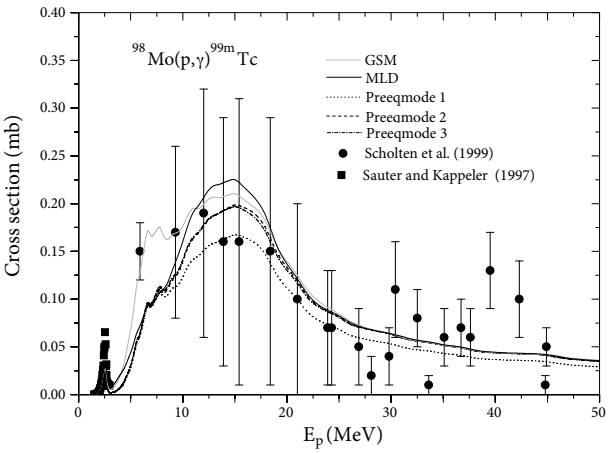

Figure 9. Comparison of excitation function of the ^{98}Mo(p,γ)^{99m}Tc reaction with experimental data [33,34].

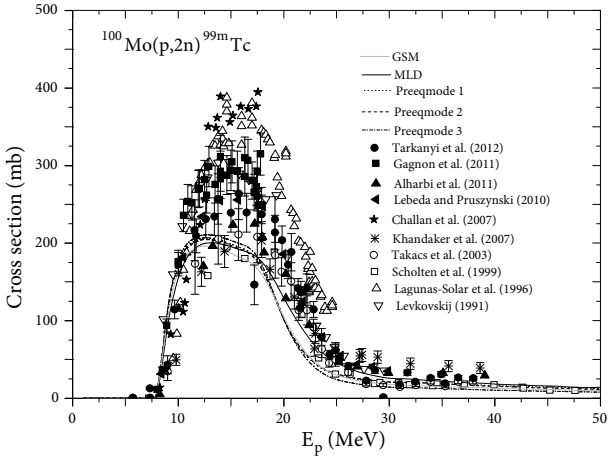

Figure 10. Comparison of excitation function of the ^{100}Mo(p,2n)^{99m}Tc reaction with experimental data [28,35–42].

et al. [37] agree with the model calculations up to 11 MeV. These measurements are higher than the theoretical calculations; however, the measurements given by Takacs et al. [38], Khandaker et al. [39], and Scholten et al. [33] are close to the theoretical excitation curve. The agreement between the experimental data [40,41] and MLD in the energy range below 12 and above 20 MeV is good. The data reported by Alharbi et al. [42] are in good agreement with the MLD beyond 18 MeV. Generally, the model calculations are consistent with each other and these results are close to the experimental data beyond 18 MeV.

4. Summary and conclusion

The cross-sectional distributions were obtained from the results of nuclear model calculations for the production of the radioisotopes ^{94m,94g,96m,96g,96,99m}Tc, some of which are used in SPECT and PET, via proton-induced reactions and were presented with the experimental data taken from EXFOR, and these results were compared to each other. The nuclear reaction model calculations, which are the GSM, MLD, and preeqmode1-3, were conducted in the Talys code for convenient excitation curves. The reason for this is that the excitation function curves are useful and important data for the thick target yields and impurity levels of radioisotopes. Therefore, in order to contribute to the nuclear data in the literature, we calculated cross-sectional data with different nuclear reaction models for proton-induced reactions on natural Mo isotopes for the production of the radioisotopes ^{94m,94g,96m,96g,96,99m}Tc.

References

[1] Audia, G.; Bersillon, O.; Blachotband, J.; Wapstra, A. H. *Nucl. Phys. A* **2003**, *729*, 3-128.

[2] Ditrói, F.; Hermanne, A.; Tárkányi, F.; Takács, S.; Ignatyuk, A. V. *Nucl. Instrum. Meth. Phys. Res. B* **2012**, *285*, 125-141.

[3] Artun, O.; Aytekin, H. *Nucl. Instrum. Meth. Phys. Res. B* **2015**, *345*, 1-8.

[4] Rösch, F.; Novgorodov, A. F.; Qaim, S. M. *Radiochim. Acta* **1994**, *64*, 113-120.

[5] Qaim, S. M. *Nucl. Med. Biol.* **2000**, *27*, 323-328.

[6] Wu, Z.; Han, Y. *Nucl. Instrum. Meth. B* **2011**, *269*, 671-684.

[7] Tarkanyi, F.; Ditroi, F.; Szelecsenyi, F.; Sonck, M.; Hermanne, A. *Nucl. Instrum. Meth. B* **2002**, *198*, 11-31.

[8] Rocco, R. J. Di; Rumsey, W. L.; Kuczynski, B. L.; Linder, K. E.; Pirro, J. P.; Narra, R. K.; Nunn, A. D. J. *J. Nucl. Mater.* **1992**, *33*, 1152-1159.

[9] Fox, R. A. *Australia's Phys. Eng. Sci. Med.* **2001**, *24*, 153-159.

[10] Qaim, S. M. In *Radiology and Nuclear Medicin*; Lahiri, S.; Nayak, D.; Mukhopadhyay, A., Eds. Saha Institute of Nuclear Physics: Kolkata, India, 2006, pp. 1-22.

[11] Maiti, M.; Dutta, B.; Lahiri, S. *Appl. Radiat. Isot.* **2010**, *68*, 42-46.

[12] Qaim, S. M.; Sudár, S.; Scholten, B.; Koning, A. J.; Coenen, H. H. *Appl. Radiat. Isot.* **2014**, *85*, 101-113.

[13] Artun, O. PhD, Department of Physics, Bülent Ecevit University, Zonguldak, Turkey, 2015.

[14] Koning, A.; Hilaire, S; Goriely, S. Talys 1.6, Manual 2013.

[15] Koning, A. J.; Duijvestijn M. C. *Nucl. Phys. A* **2004**, *744*, 15-76.

[16] Gupta, S. K. *Z. Phys. A* **1981**, *303*, 329-333.

[17] Talys package download, Talys 1.6, 2013.

[18] Aytekin, H.; Artun O.; Baldik, R. *J. Radioanal. Nucl. Chem.* **2013**, *298*, 95-103.

[19] Hoffman, R. D.; Kelley, K.; Dietrich, F. S.; Bauer, R.; Mustafa, M. Lawrence Livermore National Laboratory: UCRL-TR-211558 2005 Livermore.

[20] Griffin, J. J. *Phys. Rev. Lett.* **1966**, *17*, 478-481.

[21] Rıbansky, I.; Oblozinsky, P.; Betak, E. *Nucl. Phys. A* **1973**, *205*, 545-560.

[22] Baldik, R.; Aytekin, H.; Artun, O. *Mod. Phys. Lett. A* **2014**, *29*, 1450074.

[23] Ignatyuk, A. V.; Istekov, K. K.; Smirenkin, G. N. *Sov. J. Nucl. Phys.* **1979**, *294*, 450-454.

[24] Ignatyuk, A. V.; Weil, J. L.; Raman, S.; Kahane, S. *Phys. Rev. C* **1993**, *47*, 1504-1513.

[25] Goriely, S.; Tondeur, F.; Pearson, J. M. *Atom. Data Nucl. Data Tables* **2001**, *77*, 311-381.

[26] Exfor, Nuclear Reaction Data 2015.

[27] Rosch, F.; Qaim, S. M. *Radiochim. Acta* **1993**, *62*, 115-121.

[28] Levkovskij, V. N. *Intervesi* Moscow, Russia, 1991.

[29] Skakun, E. A.; Batij, V. G.; Rakivnenko, Yu. N.; Rastrepin, O. A. *Sov. J. Nucl. Phys.* **1987**, *46*, 17.

[30] Hogan, J. J. *Phys. Rev. C* **1972**, *6*, 810-816.

[31] Flynn, D. S.; Hershberger R. L.; Gabbard, F. *Phys. Rev. C* **1979**, *20*, 1700-1705.

[32] Zhuravlev, Yu. Yu.; Zarubin P. P.; Kolozhvari A. A. *Izv. Rossiiskoi Akademii Nauk, Ser.Fiz.* 1994, *58*, 106.

[33] Scholten, B.; Lambrecht, R. M.; Cogneau, M.; Vera R., H.; Qaim, S. M. Appl. *Radiat. Isot.* **1999**, *51*, 69-80.

[34] Sauter T.; Kappeler, F. *Phys. Rev. C* **1997**, *55*, 3127-3135.

[35] Lagunas-Solar, M.C.; Zeng, N. X.; Mirshad, I.; Grey-Morgan T. *Trans. Am. Nucl. Soc.* **1996**, *74*, 137-138.

[36] Challan, M. B.; Comsan, M. N. H.; Abou-Zeid, M. A. *J. Nucl. Radiat. Phys.* **2007**, *2*, 1-12.

[37] Gagnon, K.; Bénard, F.; Kovacs, M.; Ruth, T. J.; Schaffer, P.; Wilson, J. S.; McQuarrie, S. A. *Nucl. Med. Biol.* **2011**, *38*, 907-916.

[38] Takács, S.; Szücs, Z.; Tárkányi, F.; Hermanne, A.; Sonck, M. *J. Radioanal. Nucl. Chem.* **2003**, *257*, 195-201.

[39] Khandaker, M. U.; Uddin, M. S.; Kim, K. S.; Lee, Y. S.; Kim, G. N. *Nucl. Instrum. Methods Phys. Res. B* **2007**, *262*, 171-181.

[40] Lebeda, O.; Pruszynski, M. *Appl. Radiat. Isot.* **2010**, *68*, 2355-2365.

[41] Tárkányi, F.; Ditrói, F.; Hermanne, A.; Takács, S.; Ignatyuk, A. V. *Nucl. Instrum. Meth. B* **2012**, *280*, 45-73.

[42] Alharbi, A. A.; Azzam, A.; McCleskey, M.; Roeder, B.; Spiridon, A.; Simmons, E.; Goldberg, V. Z.; Banu, A.; Trache, L.; Tribble, R. E. In *Radioisotopes Applications in Biomedical Science*; Singh, N., Ed. InTech: Open Access, 2011, pp. 1-26.